HHS Public Access

Author manuscript

Laryngoscope. Author manuscript; available in PMC 2020 July 01.

Published in final edited form as:

Laryngoscope. 2019 July ; 129(7): E247–E254. doi:10.1002/lary.27609.

Automated quantification of vocal fold motion in a recurrent laryngeal nerve injury mouse model

Megan M Haney, DVM[1], **Ali Hamad**[2], **Emily Leary, PhD**[3], **Filiz Bunyak, PhD**[2], and **Teresa E Lever, PhD**[4]

[1]Veterinary Pathobiology, University of Missouri, Columbia, MO

[2]Electrical Engineering & Computer Science, University of Missouri, Columbia, MO

[3]Orthopaedic Biostatistics, University of Missouri, Columbia, MO

[4]Otolaryngology-Head and Neck Surgery University of Missouri, Columbia, MO

Abstract

Objectives: The goal of this study was to objectively examine vocal fold (VF) motion dynamics after iatrogenic recurrent laryngeal nerve (RLN) injury in a mouse surgical model. Furthermore, we sought to identify a method of inducing injury with a consistent recovery pattern from which we can begin to evaluate spontaneous recovery and test therapeutic interventions.

Methods: The right RLN in C57BL/6J mice was crushed for 30 seconds using an aneurysm clip with 1.3 Newtons closing force. Transoral laryngoscopy enabled visualization of VF movement prior to surgery, immediately post-crush, and at two endpoints: 3 days (n=5) and 2 weeks (n=5). VF motion was quantified with our custom motion analysis software. At each endpoint, RLN samples were collected for transmission electron microscopy (TEM) for correlation with VF motion dynamics.

Results: Our VF tracking software permitted automated quantification of several measures of VF dynamics, such as range and frequency of motion. By 2 weeks post-injury, the frequency of VF movement on the right (injured) side equaled the left, yet range of motion only partially recovered. These objective outcome measures enabled detection of VF dysfunction that persisted at 2 weeks post-crush. TEM images revealed RLN degeneration 3 days post-crush, and partial regeneration at 2 weeks, consistent with functional results obtained with automated VF tracking.

Conclusions: Our motion analysis software provides novel objective, quantitative, and repeatable metrics to detect and describe subtle VF dysfunction in mice that corresponds with underlying RLN degeneration and recovery. Adaptation of our tracking software for use with human patients is underway.

Corresponding Author: Teresa E. Lever, PhD; One Hospital Drive MA314, Columbia, MO 65212; (573)-228-0723; levert@health.missouri.edu.

Conflict of Interest: No Conflict of Interest to Disclose

Meeting Information: 121st Annual Meeting at COSM; The Triological Society; Gaylord National Resort, National Harbor, MD, USA; April 20–21, 2018

Levels of Evidence: NA

Keywords

Recurrent Laryngeal Nerve Injury; Automated Tracking; Vocal Fold Paralysis; Mouse; Objective Quantification

Introduction

Iatrogenic recurrent laryngeal nerve (RLN) injury is a common complication of anterior neck surgical procedures, such as cervical spinal surgery or thyroidectomy.[1–3] Injury to the RLN results in ipsilateral vocal fold (VF) paralysis that may contribute to dysphagia, dysphonia, and/or dyspnea (i.e., swallow, voice, and respiratory dysfunction, respectively).[4–7] These conditions are devastating for patients, especially if chronically persistent, as they are associated with poor quality of life, major depression, increased financial burden, and decreased general health.[3,7–9] Furthermore, effective treatment options to promote RLN regeneration and restore full functionality of the injured VF are lacking.[4,7,10–12]

Unfortunately, RLN injury and associated sequelae are impossible to systematically investigate in human patients. Therefore, a consistent animal model that mimics iatrogenic RLN injury is required in order to investigate the responsible mechanisms and explore potential therapeutics.[13] Indeed, work in animal models has shown that unilateral RLN injury causes ipsilateral VF paralysis, as it does in humans.[11,14–18] Though other translatable outcome measures such as voice, respiratory, and swallow function remain to be comprehensively examined, VF motion dynamics have provided robust and direct information in regard to RLN injury and subsequent recovery in these animal models. However, current methods often rely on subjective rating scales[15,16,19–21] that do not permit thorough and meticulous evaluation of VF motion dynamics. As a result, VF mobility scores may vary between observers, and minute improvements (or deteriorations) in VF motion are likely overlooked or misidentified.

Due to the inherent concerns with subjective VF analysis, efforts have been attempted to objectively quantify VF movement. One strategy involves measuring the angle between VFs during maximum abduction and maximum adduction using still-frame images.[14–16] However, angles may vary slightly within an individual animal, as total range of spontaneous VF movement during breathing depends on factors such as depth of anesthesia and ventilatory drive. Unlike human patients, anesthesia is necessary to immobilize rodent species to record VF movement. Thus, even “normal” VF movement in a single animal can vary between each laryngoscopic procedure, making longitudinal comparisons difficult with this analysis technique.

Another method for objective quantification utilizes examination of glottal area, where the area of the glottic space between midline and the VF mucosa is calculated for the injured and uninjured sides.[11,17] In this case, determining midline remains quite subjective unless there is clear visualization of both the anterior and posterior commissures, which is a challenging view to obtain in rodents. Even if midline is identified accurately, the measurements are again affected by the total range of movement of the VFs under anesthesia, which is variable between anesthetic episodes. In addition, the fluctuating

distance of the camera from the glottic space between procedures also contributes to variation in the area measured. To overcome this concern, measurements of the right VF have been compared to the left VF as a ratio to normalize VF function for each video recording.[11,17] However, this technique, as well as other manual analysis methods are time-consuming and therefore prohibitive to high-throughput data analysis in research or clinical practice.

Another major limitation of these analysis techniques is that they rely on still-frame images representing only two time points of VF movement (maximum abduction and maximum adduction), revealing little about VF motion dynamics as a whole. Therefore, with static images, it is impossible to demonstrate how the VFs are moving in relation to each other. Are the VFs moving symmetrically and in synchrony with one another? Is the motion fluid or uneven? Is there intermittent or paradoxical movement of the VFs? At what rate are the VFs moving? Is there compensation of the uninjured VF? These questions cannot be answered with still-frame images alone.

To alleviate the limitations of still-frame image analysis, we have developed custom computational video analysis software that includes two components: VFTrack and VFQuantify. VFTrack is a VF motion tracker software, whereas VFQuantify is an analytics module that computes a set of objective, quantitative outcome measures describing VF motion dynamics, enabling objective comparisons across time and populations. These measures quantify aspects of motion behavior pertaining to healthy and paralyzed VFs, such as amplitude, frequency, range, symmetry, etc. In this study, two measures, Mean Motion Range Ratio (MMRR) and Open Close Cycle Ratio (OCCR), were developed to begin to objectively assess VF motion dynamics. VFQuantify was also used to calculate the maximum angle of abduction and the minimum angle during adduction to correlate our findings with previous techniques described in the literature.

To accomplish our primary objective (i.e., demonstration of the utility of our VFTrack and VFQuantify software), we produced a unilateral RLN compression (crush) injury in a mouse model using an aneurysm clip to induce ipsilateral VF dysfunction.[19–23] To visualize VF motion, transoral laryngoscopy was performed prior to and immediately following crush injury, as well as 3 days and 2 weeks post-crush. Our secondary objective was to confirm that this nerve crush methodology and severity of force produces unilateral VF immobility in mice, and to characterize how VF function recovers over time without treatment. In addition to functional analysis, we performed transmission electron microscopy (TEM) to document nerve pathology at each respective endpoint.

Materials and Methods

Ten C57BL/6J (B6) mice (n=4 males; 6 females), approximately 4 months of age, were used for this study, which was approved by our Institutional Animal Care and Use Committee. Mice were group housed by sex on a 12:12 light/dark cycle using individually ventilated cages, and had free access to food and water.

RLN crush injury procedure:

Mice were anesthetized using a ketamine-xylazine cocktail (90;11.25 mg/kg), prepared aseptically for surgery, and placed in dorsal recumbency on a customized platform under a surgical microscope. A midline incision (~1–2 cm) was made on the ventral neck, and the salivary glands were retracted laterally to expose the strap muscles overlying the trachea. The right RLN was gently isolated at the level of the 5th tracheal ring and crushed with a Sugita Titanium aneurysm clip (Mizuho, Tokyo, Japan)[19,20,22,23] with a 1.3 N manufacturer-calibrated closing force. The aneurysm clip was closed for 30 seconds to induce a 1 mm injury[24] in all mice (Figure 1). The left RLN served as an internal control for this study.

Transoral Laryngoscopy:

Transoral laryngoscopy[25] was performed immediately prior to surgical incision, while the mice were anesthetized, positioned in dorsal recumbency, and immobilized in ear bars. To do so, the tongue was retracted with a cotton swab and gentle finger-grip, and a micromanipulator-controlled sialendoscope with a customized laryngoscope sheath was gently inserted into the oral cavity to visualize baseline VF movement. In mice, VF movement is spontaneous with breathing, rather than an evoked response. Immediately post-crush, laryngoscopy was performed again to confirm ipsilateral VF paralysis. After repeat laryngoscopy, the incision was sutured closed, and the mouse was recovered. Laryngoscopy was performed once more at 3 days post-crush (n=5) or 2 weeks post-crush (n=5), prior to euthanasia and tissue collection. Laryngoscopy video recordings (30 frames per second; approximately 1–3 minutes long) were subjectively analyzed by two trained, blinded reviewers using a Likert scoring system (0 = no VF movement, 1 = partial VF movement, 2 = normal VF movement).[15,19–21] Additionally, VF movement was tracked bilaterally with our automated motion tracking software, VFTrack. Then VFQuantify was used to measure amplitude- and frequency- based outcome metrics, MMRR and OCCR, respectively, along with VF angle during maximum abduction and adduction, described below.

Automated Analysis with VFTrack and VFQuantify:

Our custom, VF motion analytics software package was used to analyze VF motion dynamics. A 10 second clip was selected from each video recording, based on adequate visualization of the VFs and no aberrant camera movement. On the first video frame in each clip, a pair of points was manually placed on each VF (VF-glottal region boundary) for automated tracking over time using our VFTrack software. Point selection was based on the anatomical structure of the VFs, which were selected on the upper (i.e., ventral) half of each VF to ensure higher sensitivity to small VF motions. Because of the V-shaped nature of the VFs, VF points with higher y coordinates result in larger displacements for the same angular motion. Left (L_L) and right (L_R) lines were automatically passed through each pair of tracked points to approximate the medial side of the VF and the ipsilateral arytenoid cartilage in each video frame (Figure 2a). Three points of interest (p_o, p_L, p_R) were automatically located on the two VF lines (L_L and L_R) in each frame. P_o was the intersection point of the two VF lines, typically located midline, dorsal to the arytenoid cartilages, and p_L and p_R were two points on L_L and L_R, each at the same fixed distance from p_o (determined as the largest distance between the tracked points and p_o) (Figure 2a). Left and right VF

motion ranges and corresponding motion midlines were automatically computed based on displacement (in pixels) of points p_L and p_R (Figure 2b). VF motion was automatically calculated through displacement of points p_L and p_R with respect to their motion midlines and graphically displayed as a cyclic waveform due to the oscillatory motion of the VFs during breathing (Figure 3).

Using VFQuantify, motion behavior differences between left and right VFs were measured using two complementary ratios, OCCR (Open Close Cycle Ratio) and MMRR (Mean Motion Range Ratio), to characterize the frequency and amplitude of VF motion, respectively. The number of motion cycles for each VF was computed as the number of motion midline crossings. OCCR was then computed as the ratio of number of motion cycles for right and left VFs. Motion range of each VF was defined as the distance between the left-most and right-most positions of the VF (i.e., local minima and maxima in Figure 3) for each cycle. Mean Motion Range (MMR) was computed by averaging motion ranges over all time periods (i.e., each VF cycle within the 10 s video clip). MMRR was defined as MMR_{right}/MMR_{left}, which compares right and left VF motion amplitudes. The described point selection protocol [$p_L(t)$, $p_R(t)$ equidistant from $p_0(t)$] and unitless MMRR ensure robustness against variations in VF size across different subjects and camera distance from the VFs. In addition, the two VF lines, L_L and L_R, were used for automated measurement of VF angle during maximum abduction (maximum angle) and maximum adduction (minimum angle) for each video, without needing to manually acquire still images. The angular range of VF movement for each mouse was calculated by subtracting the minimum angle from the maximum angle measurements.

VFTrack Validation and Performance Evaluation:

We validated tracking accuracy of our VFTrack software by comparing the automatically generated tracks from VFTrack to manually generated tracks by two independent reviewers (MH and TL) on a subset of videos (2 out of 5 videos per time point). For each selected video, manual tracks were generated by selecting a point (x-y coordinate) on each VF boundary and sequentially marking the same boundary coordinate on every frame of each video. Given that different points can be manually selected and tracked on the VF boundary to produce the same line used to compute our outcome measures (MMRR and OCCR), reviewers were asked to track only the x-coordinate on the VF boundary in each frame. The y-coordinate was automatically displayed on each frame, indicated by a blue horizontal line spanning the image. MMRR and OCCR measures were calculated for each video based on the manual points (n=600 per video) placed by each reviewer. VFTrack performance was evaluated by computing (1) the pixel distance between manually and automatically tracked points along the VF boundary; (2) differences in MMRR and OCCR measures produced by these points; and (3) the time needed to generate these points. In addition, VFTrack was ran twice more by two independent reviewers to verify its reliability between reviewers.

TEM:

Mice were perfused with saline followed by 4% paraformaldehyde (PFA). RLNs were dissected *en bloc* and post-fixed in 4% PFA / 2% glutaraldehyde in 100 mM sodium cacodylate buffer. Samples were sent to our Electron Microscopy Core for standard tissue

processing, embedding, and sectioning (85 nm). High resolution TEM cross-sectional images from the left and right RLNs distal to the crush-site were obtained using a JEOL JEM 1400 TEM microscope at 80 kV with a Gatan Ultrascan 1000 CCD camera.

Statistics:

Mice were divided into two groups based on endpoint. Change scores between baseline and endpoint were calculated, and independent samples T-tests were used to separately analyze both outcome metrics (MMRR and OCCR). Spearman's correlations were utilized to compare subjective (Likert scale) and all objective outcome measures (MMRR, OCCR, and VF angle). Pearson's correlations were computed between the calculated angular range of motion and MMRR, to compare traditional objective analysis techniques with our novel objective metrics. Statistics were computed using IBM SPSS Statistics 24 and p values of less than 0.05 were considered significant.

Results

Subjective VF Motion Results:

All mice survived the RLN crush surgical procedure and subsequent laryngoscopy recordings. Our subjective analysis of laryngoscopy video recordings revealed that all mice (n=10) had normal, bilaterally-symmetrical VF motion (score = 2) prior to injury. Immediately post-crush, all mice developed complete right-sided (ipsilateral) VF paralysis (score = 0). At the 3 days post-crush endpoint, the right VF remained immobile in all 5 mice. In contrast, mice had partial to full recovery of right VF movement at 2 weeks post crush (n=5; average score = 1.4; std = 0.55) (Figure 4a).

Objective VF Motion Results:

Due to variable total range of VF motion in individual mice between anesthetic episodes, right VF movement was compared to left VF movement and quantified as a ratio (right:left) for our objective outcome measures. Our amplitude-based measure, Mean Motion Range Ratio (MMRR), allows quantification of right (injured) versus left (control) VF range of motion. Our frequency-based measure, Open Close Cycle Ratio (OCCR), quantifies the number of right VF movements compared to the left. At baseline, ratios for both MMRR and OCCR were near 1, signifying that right VF motion dynamics were similar to the left. Immediately post-crush, ratios were virtually 0, indicating complete paralysis of the right VF. At 3 days post-crush, MMRR and OCCR remained near 0, suggesting minimal to no recovery. By 2 weeks, our findings revealed partial recovery of VF range of motion and full recovery of VF frequency (Figure 4b and 4c). Mice at 3 days and 2 weeks post-crush had significantly different change scores for both outcome metrics. In addition, our automated VF angle measurements (Figure 4d) correlated with MMRR outcomes, signifying our novel, automated MMRR metric corresponds with previously reported angle measurement methods that are based on time consuming analysis of still-frame images.[14–16] Correlations between outcome measures are displayed in Tables 1 and 2. In summary, our automated outcome measures, MMRR and OCCR, had statistically significant correlation with our subjective analysis, as well as with angular range of motion, indicating our novel outcome measure

detect similar changes as with historic analysis methods, while providing more objective and informative outcome metrics that can be expanded upon in future studies.

VFTrack Validation and Performance Evaluation:

To validate our automated tracking software, two reviewers performed manual, frame-by-frame analysis on a subset of videos. The average pixel distance between the automated software and each independent reviewer was 1.94 pixels (sd = 1.16; MH) and 1.88 pixels (sd = 1.10; TL). The average pixel distance between reviewers was 1.59 pixels (sd = 0.40). Figure 5 displays a representative image of pixel error in a single video frame between each reviewer and VFTrack. On average, it took approximately 18 minutes longer to manually track the two VF boundary points compared to our automated process. Thus, VFTrack drastically decreases the time to collect the MMRR and OCCR measures reported in this study. Calculations of these measures were performed the same for both manual and automated tracks using our VFQuantify software. The average difference in MMRR and OCCR was less than 0.09 and 0.20, respectively, for all three cases. The larger error in OCCR was likely due to inconsistent point selection with manual analysis. Additionally, MMRR and OCCR results did not significantly change when VFTrack was reran by two different reviewers.

TEM:

Cross-sections of the left (control) RLN in all mice revealed thick axonal myelination with minimal interstitial space between axons. In contrast, there was evidence of extensive axonal degeneration in the right RLN at 3 days post-crush. This degeneration was indicated by collapsed nerve fibers and dense, compressed myelin debris. At 2 weeks post-crush, the presence of thinly myelinated axons provided evidence of nerve regeneration (Figure 6).

Discussion

The results from this study show that an aneurysm clip induced method of unilateral RLN compression injury resulted in ipsilateral VF impairment that allowed partial recovery by 2 weeks post-crush. This recovery was objectively evaluated with our custom VF motion analytics software, VFTrack and VFQuantify, to provide novel outcome metrics to detect and quantify subtle changes in VF motion in mice after RLN injury. Our primary objective was to demonstrate the feasibility of our novel software by comparing outcome metrics with previously described methods (i.e., objective angle measurements and subjective scoring). Thus, we have shown that our software can achieve similar results as currently used methods; however, it does so via automated objective quantification methods, enabling efficient analysis of a high volume of dynamic VF motion recordings, rather than single frame analysis.

The subjective VF recovery results found in this study correlated with the objective measures obtained by our software, which were further validated by semi-automated manual analysis methods. However, our objective measures provide more precise and accurate metrics to quantify longitudinal VF recovery. Not only can our motion analysis software detect the difference between paralyzed and fully functional VFs, but it can detect small, but

perhaps clinically important, changes in VF motion. Without VFTrack and VFQuantify, it would be extremely challenging and time consuming to calculate the novel functional outcome measures identified in this study, mean motion range ratio (MMRR) and open close cycle ratio (OCCR). Additionally, with our objective VF tracking there is less variation between mice in each group when compared to subjective scoring methods, which increases the likelihood of detecting significant findings when evaluating different treatments and time points.

Objective tracking allows full visualization of VF motion dynamics throughout the entire video clip, thus overcoming the limitation of quantifying static images at only two positions in the respiratory cycle. The data supplied by our motion analysis software includes both raw measures along with the ratios of right VF dynamics compared to the left. In addition to the metrics quantified in this study, we are searching for additional robust outcome measures that may provide new or complementary information for improved diagnostics and treatment evaluation. These measures can be used to acquire more meaningful information beyond basic range of motion and quantification of VF angles at maximum adduction and abduction. Possible automated metrics of VF motion dynamics include: rate of VF movement, fluidity of VF motion, VF length/size/area, the amount of VF jitter, and uninjured VF compensation, among many others.

Our VF motion software is a crucial asset for objective and reproducible analysis of VF movement for experimental purposes, but it may have much broader applications beyond a laboratory setting. In fact, we are currently working on using this technology to quantify VF motion dynamics in healthy human patients, along with patients with known laryngeal dysfunction. Besides tracking VF movement with respiration, we have begun tracking more complex laryngeal functions, including the laryngeal adductor reflex and other behavioral tasks, such as sniffing through the nose, taking a deep breath, holding the breath, and vocal diadochokinetic tasks. Once perfected and validated, healthcare professionals can begin to use VFTrack and VFQuantify in a clinical setting in real time to advance diagnostic capabilities. We hope this will allow healthcare professionals to better monitor disease progression and treatment effects over time, enabling them to tailor therapeutic approaches to distinct symptoms and objectively quantify treatment efficacy in individual patients.

Conclusions

In conclusion, subjective analysis remains crucial for investigators to estimate VF motion dynamics. However, because subjective analysis is inadequate for detecting small changes in VF motion over time, objective, quantitative measures are needed to fully and accurately assess VF motion dynamics. Furthermore, automation of VF motion quantification allows for high through-put analysis of dynamic VF motion recordings, enabling increased, highly-efficient research with our animal models. Most important, we have been expanding our software capabilities to identify additional outcome metrics that are amenable to automation, and are also clinically relevant (i.e., translatable to humans). As such, our software is currently being tested with human patients to improve diagnosis of VF disorders and enhance monitoring of treatment efficacy.

Acknowledgements

We would like to thank Kate Osman for managing our lab and caring for our mouse colony on campus. We would also like to acknowledge our funding sources: vocal fold motion tracking software (Coulter Translational Partnership) and post-doctoral training stipend & supplies (NIH T32–5T32OD011126–39).

References

1. Liu JB, Sosa JA, Grogan RH, et al. Variation of Thyroidectomy-Specific Outcomes Among Hospitals and Their Association With Risk Adjustment and Hospital Performance. JAMA surgery. 2018;153(1):e174593. [PubMed: 29188293]
2. Chen C-C, Huang Y-C, Lee S-T, Chen J-F, Wu C-T, Tu P-H. Long-term result of vocal cord paralysis after anterior cervical disectomy. European Spine Journal. 2014;23(3):622–626. [PubMed: 24212479]
3. Ta JH, Liu YF, Krishna P. Medicolegal Aspects of Iatrogenic Dysphonia and Recurrent Laryngeal Nerve Injury. Otolaryngol Head Neck Surg. 2016;154(1):80–86. [PubMed: 26419840]
4. Rosko AJ, Kupfer RA, Oh SS, Haring CT, Feldman EL, Hogikyan ND. Immunohistologic analysis of spontaneous recurrent laryngeal nerve reinnervation in a rat model. Laryngoscope. 2018;128(3):E117–e122. [PubMed: 29226485]
5. Brunner E, Friedrich G, Kiesler K, Chibidziura-Priesching J, Gugatschka M. Subjective breathing impairment in unilateral vocal fold paralysis. Folia phoniatrica et logopaedica : official organ of the International Association of Logopedics and Phoniatrics (IALP). 2011;63(3):142–146. [PubMed: 20938194]
6. Mattsson P, Hydman J, Svensson M. Recovery of laryngeal function after intraoperative injury to the recurrent laryngeal nerve. Gland Surg. 2015;4(1):27–35. [PubMed: 25713777]
7. Chandrasekhar SS, Randolph GW, Seidman MD, et al. Clinical practice guideline: improving voice outcomes after thyroid surgery. Otolaryngol Head Neck Surg. 2013;148(6 Suppl):S1–37.
8. Fang TJ, Li HY, Gliklich RE, Chen YH, Wang PC, Chuang HF. Quality of life measures and predictors for adults with unilateral vocal cord paralysis. Laryngoscope. 2008;118(10):1837–1841. [PubMed: 18806475]
9. Wang W, Chen D, Chen S, et al. Laryngeal Reinnervation Using Ansa Cervicalis for Thyroid Surgery-Related Unilateral Vocal Fold Paralysis: A Long-Term Outcome Analysis of 237 Cases. PLoS ONE. 2011;6(4):e19128. [PubMed: 21559458]
10. Lin RJ, Smith LJ, Munin MC, Sridharan S, Rosen CA. Innervation status in chronic vocal fold paralysis and implications for laryngeal reinnervation. The Laryngoscope.n/a-n/a.
11. Choi JS, Oh SH, An HY, Kim YM, Lee JH, Lim JY. Functional regeneration of recurrent laryngeal nerve injury during thyroid surgery using an asymmetrically porous nerve guide conduit in an animal model. Thyroid. 2014;24(1):52–59. [PubMed: 24015805]
12. Wang B, Yuan J, Xu J, Xie J, Wang G, Dong P. Neurotrophin expression and laryngeal muscle pathophysiology following recurrent laryngeal nerve transection. Mol Med Rep. 2016;13(2):1234–1242. [PubMed: 26677138]
13. Paniello RC, Rich JT, Debnath NL. Laryngeal Adductor Function in Experimental Models of Recurrent Laryngeal Nerve Injury. The Laryngoscope. 2015;125(2):E67–E72. [PubMed: 25283381]
14. Hernandez-Morato I, Sharma S, Pitman MJ. Changes in neurotrophic factors of adult rat laryngeal muscles during nerve regeneration. Neuroscience. 2016;333:44–53. [PubMed: 27421227]
15. Hernandez-Morato I, Valderrama-Canales FJ, Berdugo G, et al. Reorganization of laryngeal motoneurons after crush injury in the recurrent laryngeal nerve of the rat. J Anat. 2013;222(4):451–461. [PubMed: 23444899]
16. Wang B, Yuan J, Chen X, Xu J, Li Y, Dong P. Functional regeneration of the transected recurrent laryngeal nerve using a collagen scaffold loaded with laminin and laminin-binding BDNF and GDNF. Scientific reports. 2016;6:32292. [PubMed: 27558932]
17. Nishimoto K, Kumai Y, Yumoto E. Paradoxical movement of rat vocal folds following recurrent laryngeal nerve injury. Acta oto-laryngologica. 2014;134(11):1164–1171. [PubMed: 25315916]

18. Abstracts of Scientific Papers 2017 AALAS National Meeting. Journal of the American Association for Laboratory Animal Science. 2017;56(5):574–694. [PubMed: 28903831]
19. Tessema B, Pitman MJ, Roark RM, Berzofsky C, Sharma S, Schaefer SD. Evaluation of functional recovery of recurrent laryngeal nerve using transoral laryngeal bipolar electromyography: a rat model. The Annals of otology, rhinology, and laryngology. 2008;117(8):604–608.
20. Tessema B, Roark RM, Pitman MJ, Weissbrod P, Sharma S, Schaefer SD. Observations of recurrent laryngeal nerve injury and recovery using a rat model. Laryngoscope. 2009;119(8):1644–1651. [PubMed: 19504559]
21. Monaco GN, Brown TJ, Burgette RC, et al. Electrical stimulation and testosterone enhance recovery from recurrent laryngeal nerve crush. Restor Neurol Neurosci. 2015;33(4):571–578. [PubMed: 23902984]
22. Sarikcioglu L, Demir N, Demirtop A. A standardized method to create optic nerve crush: Yasargil aneurysm clip. Experimental eye research. 2007;84(2):373–377. [PubMed: 17157296]
23. Sarikcioglu L, Ozkan O. Yasargil-Phynox aneurysm clip: a simple and reliable device for making a peripheral nerve injury. Int J Neurosci. 2003;113(4):455–464. [PubMed: 12856475]
24. Bridge PM, Ball DJ, Mackinnon SE, et al. Nerve crush injuries--a model for axonotmesis. Experimental neurology. 1994;127(2):284–290. [PubMed: 8033968]
25. Shock LA, Gallemore BC, Hinkel CJ, et al. Improving the Utility of Laryngeal Adductor Reflex Testing: A Translational Tale of Mice and Men. Otolaryngol Head Neck Surg. 2015;153(1):94–101. [PubMed: 25832829]

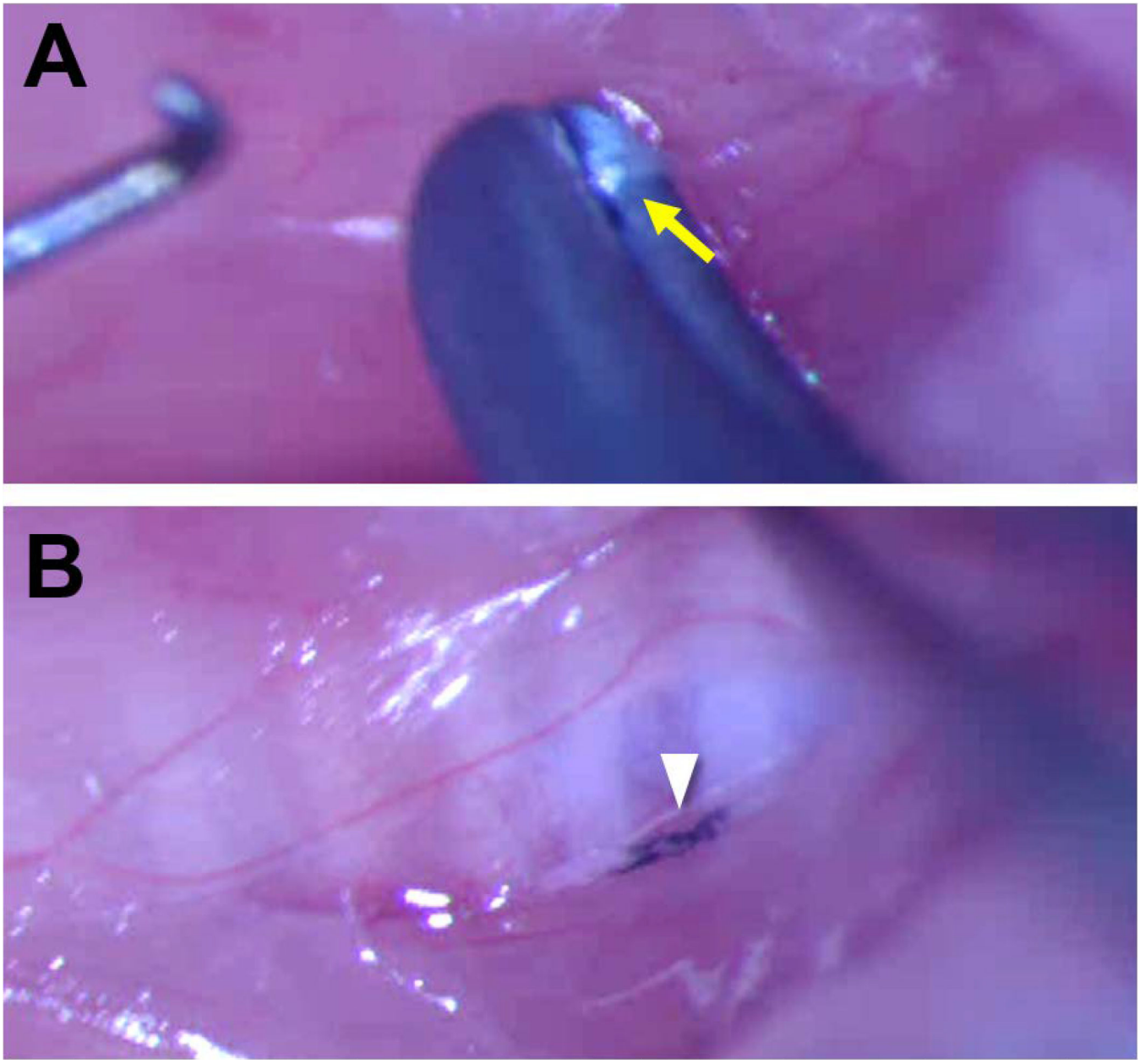

Figure 1:

A Sugita Titanium aneurysm clip with a 1.3 N closing force was used to crush the right RLN in all mice at the level of the 5th tracheal ring. A) The aneurysm clip (1 mm wide) was closed for 30 seconds to induce injury. Arrow indicates the RLN. B) Ultraviolet sterilized carbon powder was placed on the crush tool to mark the site of injury on the RLN for post-mortem identification, indicated by arrowhead. The right strap muscle is retracted laterally to allow visualization of the RLN.

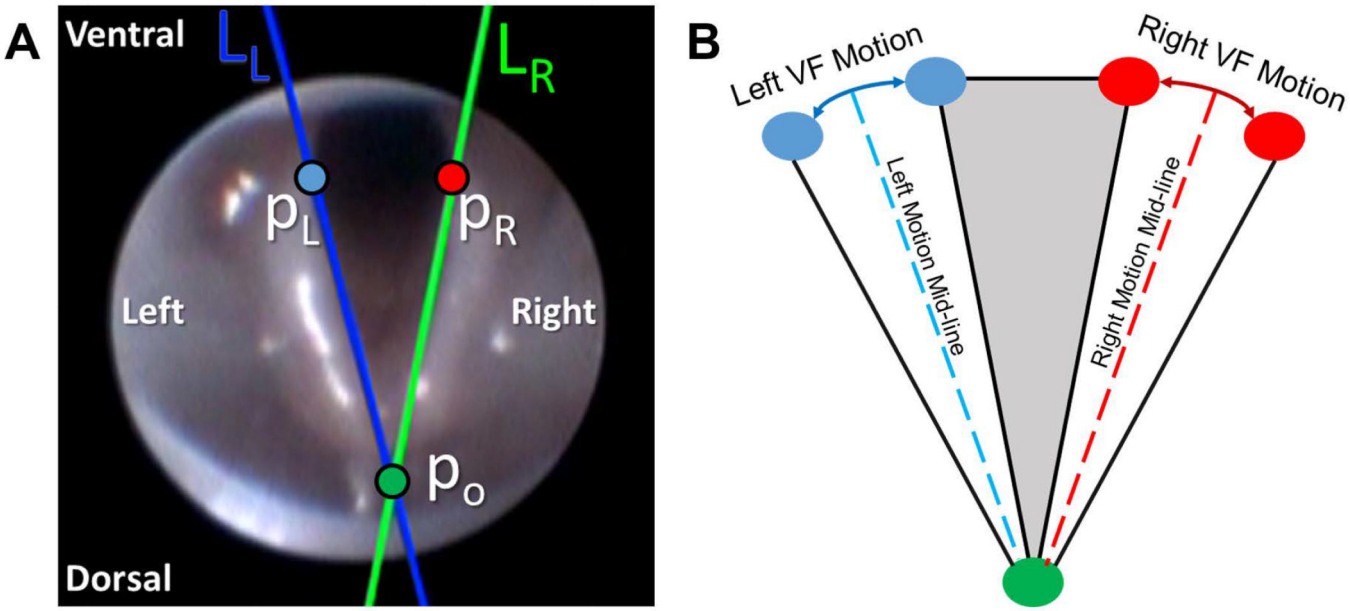

Figure 2:

A) Automatically tracked VF lines (L_L and L_R) and points of interest (p_o, p_L, p_R) shown on a sample video frame. B) Illustration of left/right VF motion ranges and associated motion mid-lines.

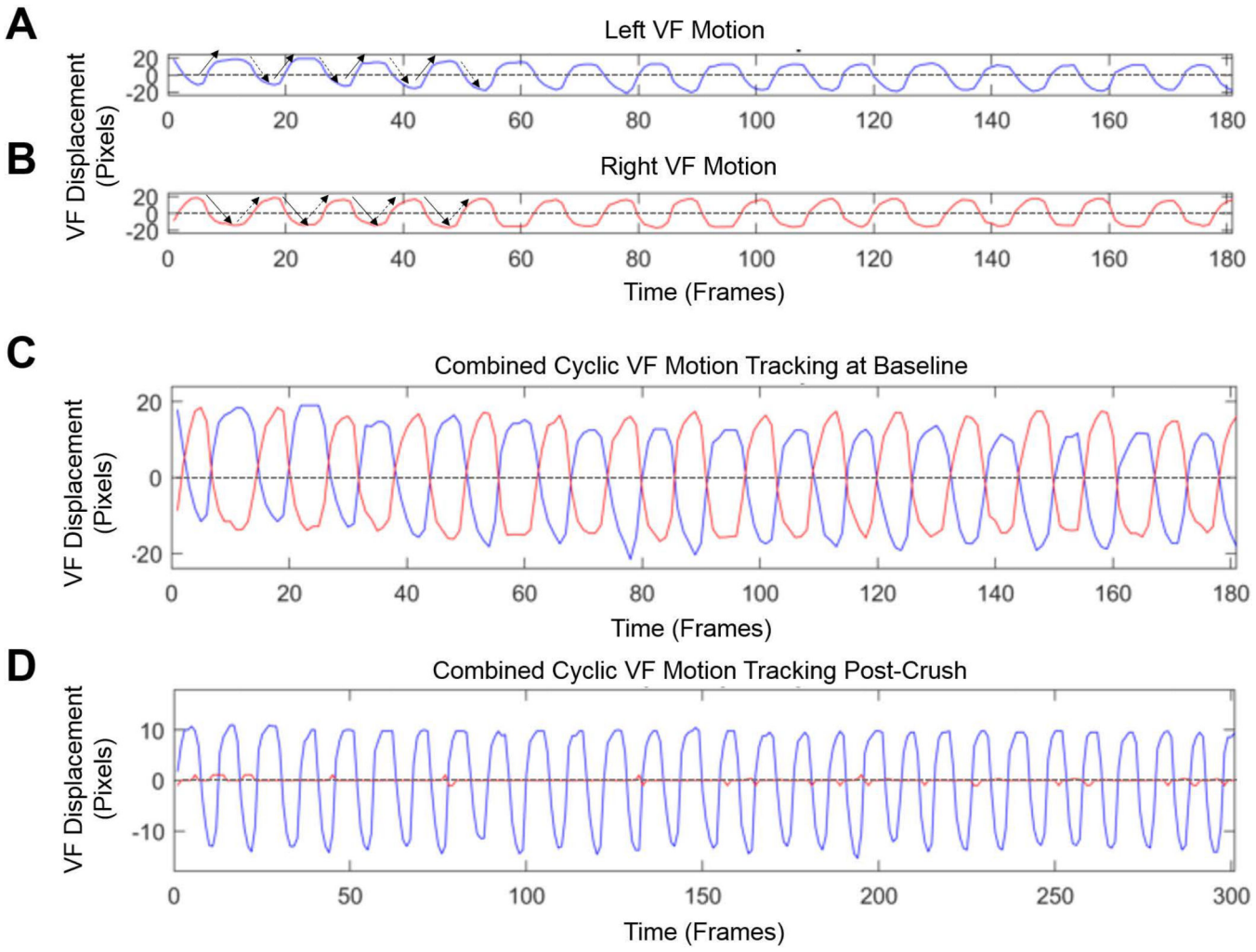

Figure 3:

A & B) Displacement of the left (blue) and right (red) VFs individually over time. The x-axis is the video frame number and the y-axis is VF displacement measured in pixels. The graphs display the cyclic movement as the VFs oscillate back and forth across their respective motion midlines (dashed-lines) during inspiration and expiration in a normal mouse at baseline under a surgical level of anesthesia. Solid arrows indicate the VF is adducting (closing), whereas dashed arrows indicate the VF is in a state of abduction (opening). C) The left and right VF displacement graphs from baseline are overlaid with respect to their motion midlines. Right VF range and frequency of motion are similar to the left. D) Combined right and left VF movement immediately after a right RLN crush injury. There is no right VF movement, compared to normal left VF movement.

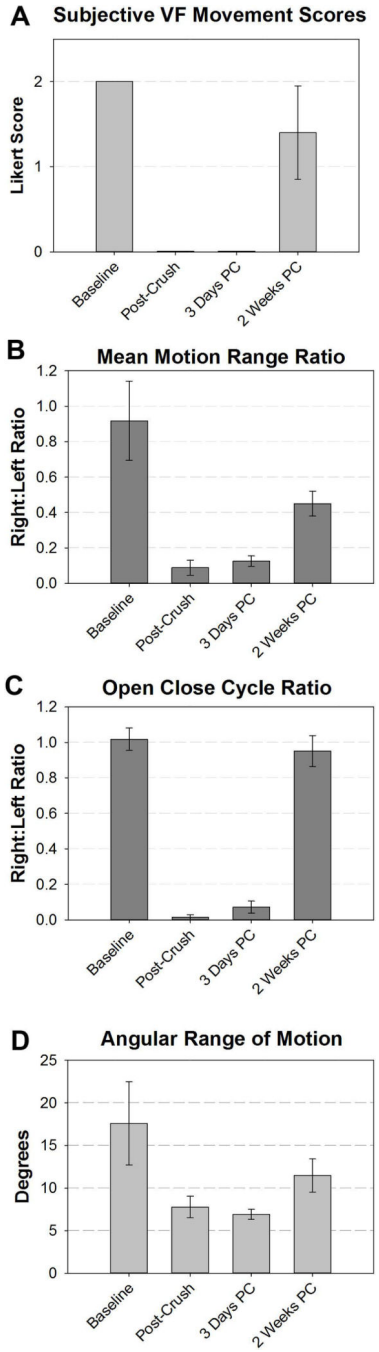

Figure 4:

VF motion was quantified using subjective 4A) and objective 4B-D) outcome metrics. In all cases, VF motion was impaired by the RLN crush injury, which partially recovered by 2 weeks post crush. One video file (immediately post-crush) had poor image quality for automated tracking and was excluded from graphical analysis in 4B and C.

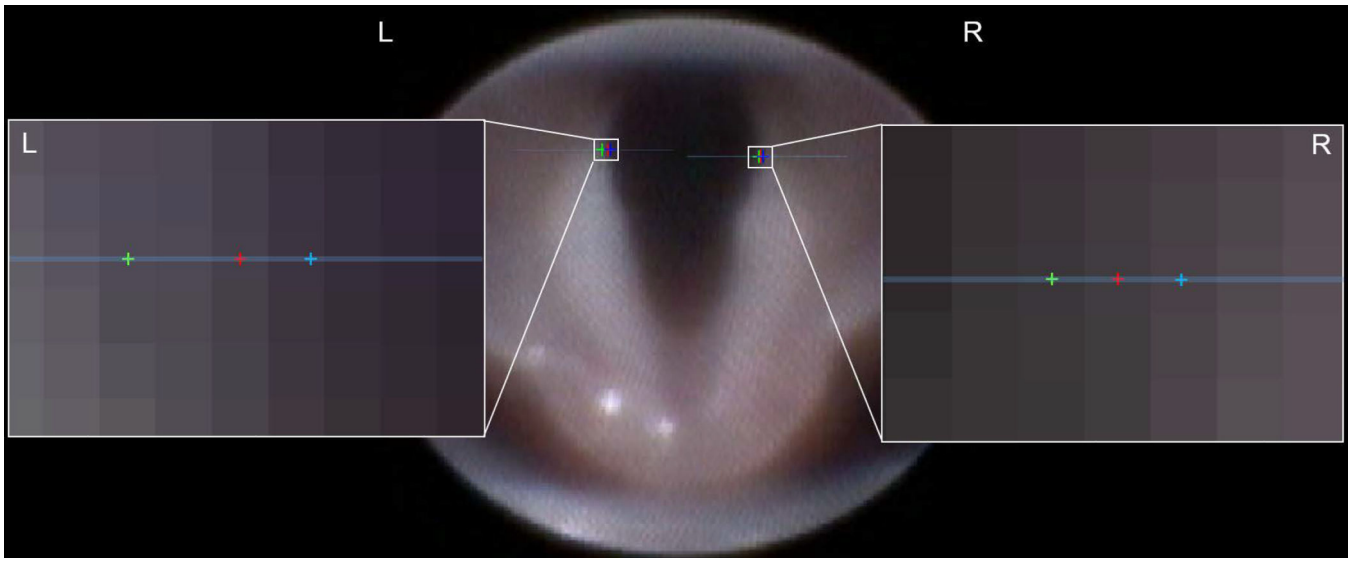

Figure 5:

Representative image of VFTrack validation process. Vocal fold (VF) boundaries were tracked with our automated software (red points). Manual points were placed on each frame by two independent reviewers (green and blue points). The expanded view of the left and right VF boundaries shows individual pixels and the pixel location of each point along the given blue horizontal line. In this image, both reviewers are no more than two pixels away from the automatically tracked point, demonstrating high reliability of our automated tracking software. For perspective, the total endoscopy field of view contains approximately 60,000 pixels.

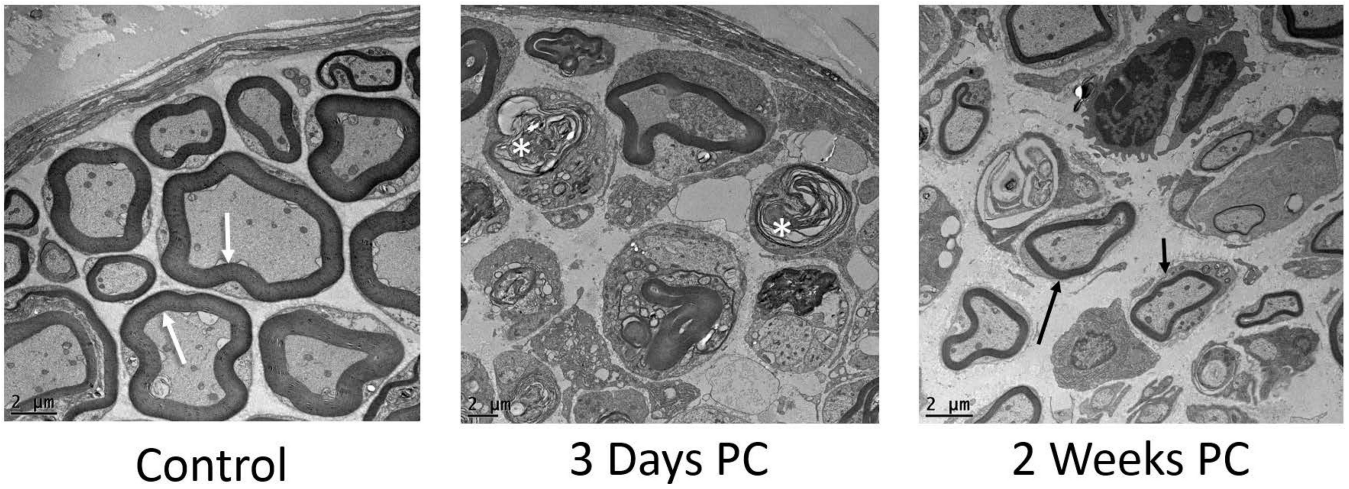

Figure 6:

Representative TEM images of control and experimental RLN (above; 1200x). Left (control) nerves showed thick myelination (white arrows) and tightly packed axons. At 3 days post-crush, the right (experimental) RLN showed extensive signs of degeneration, indicated by collapsed fibers and dense, compressed myelin debris (asterisks). At 2 weeks post-crush, regeneration of thinly myelinated axons was evident (arrows) within an expanded perineurial space.

Table 1.

Associations between subjective and objective VF measures using Spearman's correlation.

		MMRR	OCCR	Angular Range of Motion
Subjective Score (n=30)	Correlation Coefficient	0.874**	0.824**	0.886**

** Correlation is significant at the 0.0001 level (2-tailed).

MMRR = Mean Motion Range Ratio; OCCR = Open Close Cycle Ratio

Table 2.

Associations between objective measures of VF motion using Pearson correlations.

		MMRR	CR	Angular Range of Motion
MMRR (n=30)	Pearson Correlation	1	0.799**	0.817**
CR (n=30)	Pearson Correlation	0.799**	1	0.686**
Angular Range of Motion (n=30)	Pearson Correlation	0.817**	0.686**	1

** Correlation is significant at the 0.0001 level (2-tailed).

MMRR = Mean Motion Range Ratio; OCCR = Open Close Cycle Ratio